

**Supporting information for: Spin-State Effects on the
Thermal Dihydrogen Release from Solid-State
[MH(η^2 -H₂)dppe₂]⁺ (M = Fe, Ru, Os) Organometallic
Complexes for Hydrogen Storage Applications**

David G. Abrecht, Jorge A. Muñoz, Hillary L. Smith, and Brent Fultz*

*W.M. Keck Laboratory, California Institute of Technology, 1200 E. California Blvd, MC 138-78,
Pasadena, CA 91125*

E-mail: btf@caltech.edu

*To whom correspondence should be addressed

Contents

Figure S.1	Mass Spectrograph of Initial Degassing of [FeH(η^2 -H ₂)dppe ₂][NTf ₂] . . .	S3
Figure S.2	Mass Spectrograph of Hydrogen Cycling onto [FeH(η^2 -H ₂)dppe ₂][NTf ₂] .	S4
Figure S.3	Relaxed structure of singlet [FeHdppe ₂] ⁺	S5
Figure S.4	Relaxed Structure of Triplet [FeHdppe ₂] ⁺	S6
Figure S.5	Relaxed Structure of [FeH(η^2 -H ₂)dppe ₂] ⁺	S7
Table 1	Calculated Energies of Molecular Fragments	S8
Table 2	SCS-MP2 Calculated Energies of Molecular Fragments	S10

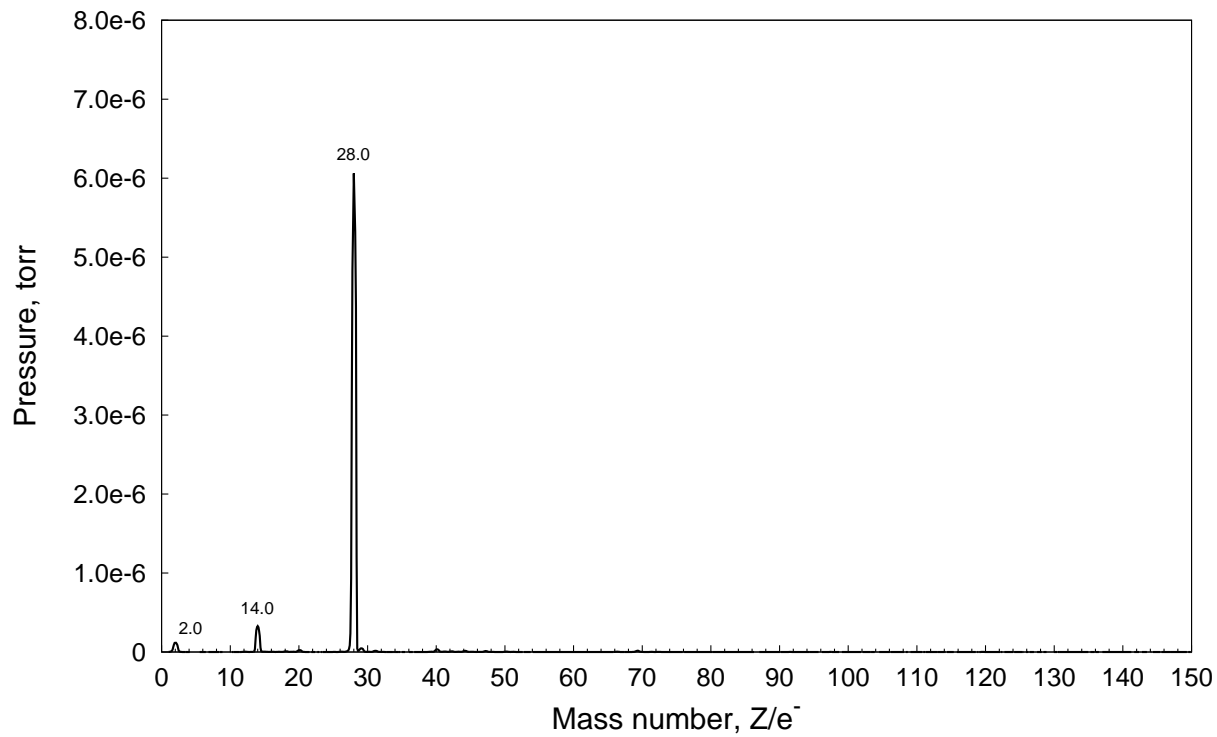


Figure S.1: Residual mass spectrograph of the initial degassing of as-synthesized $[\text{FeH}(\eta^2\text{-H}_2)\text{dppe}_2]\text{[NTf}_2]$ containing N_2 contamination at the binding site. Degassing occurred from the solid state under vacuum conditions at 393K, and shows the preferential loss of N_2 gas from the species.

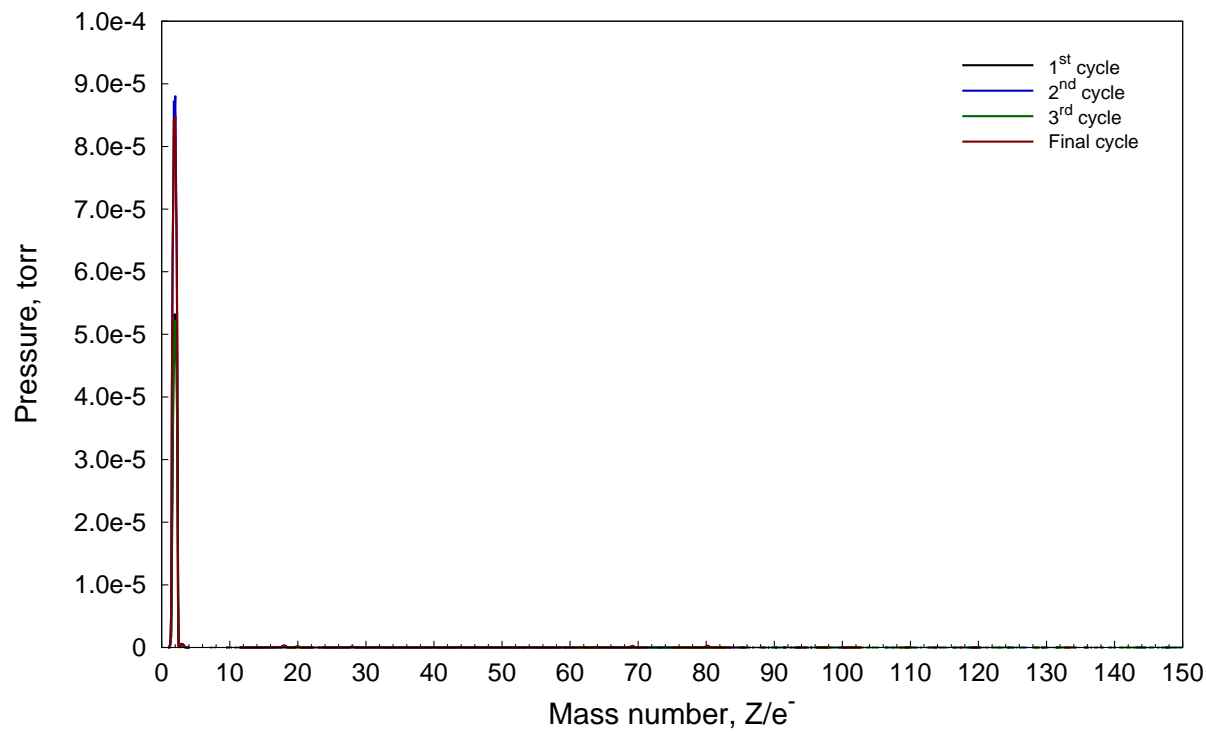


Figure S.2: Residual mass spectrograph of the volatile thermal decomposition products of $[\text{FeH}(\eta^2\text{-H}_2)\text{dppe}_2][\text{NTf}_2]$ during hydrogen cycling at 413 K. Hydrogen gas is the only observed decomposition product from the material after for all four hydrogenation/dehydrogenation cycles.

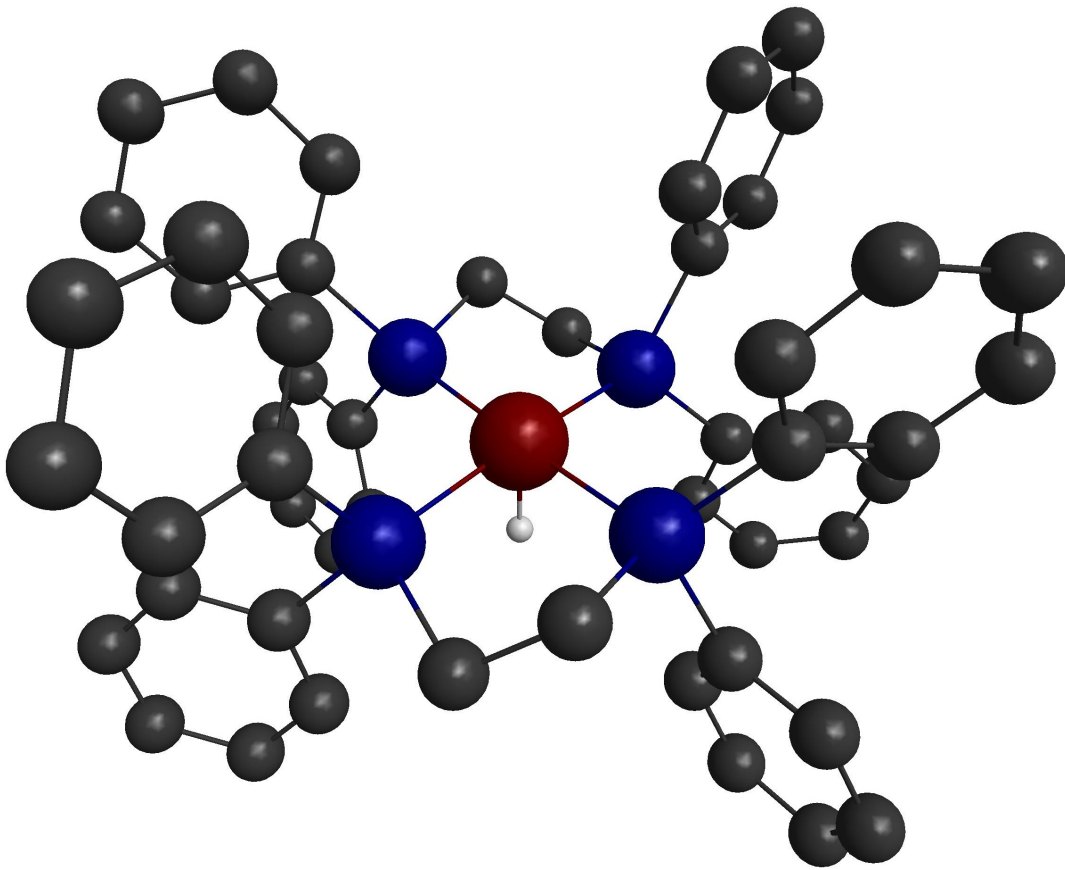


Figure S.3: Optimized structure of the singlet state organometallic fragment $[\text{FeHdppe}_2]^+$ using the UHF approximation and LANL2DZ-ECP basis sets, showing typical octahedral geometry. Alkyl and aryl hydrogens have been omitted for clarity.

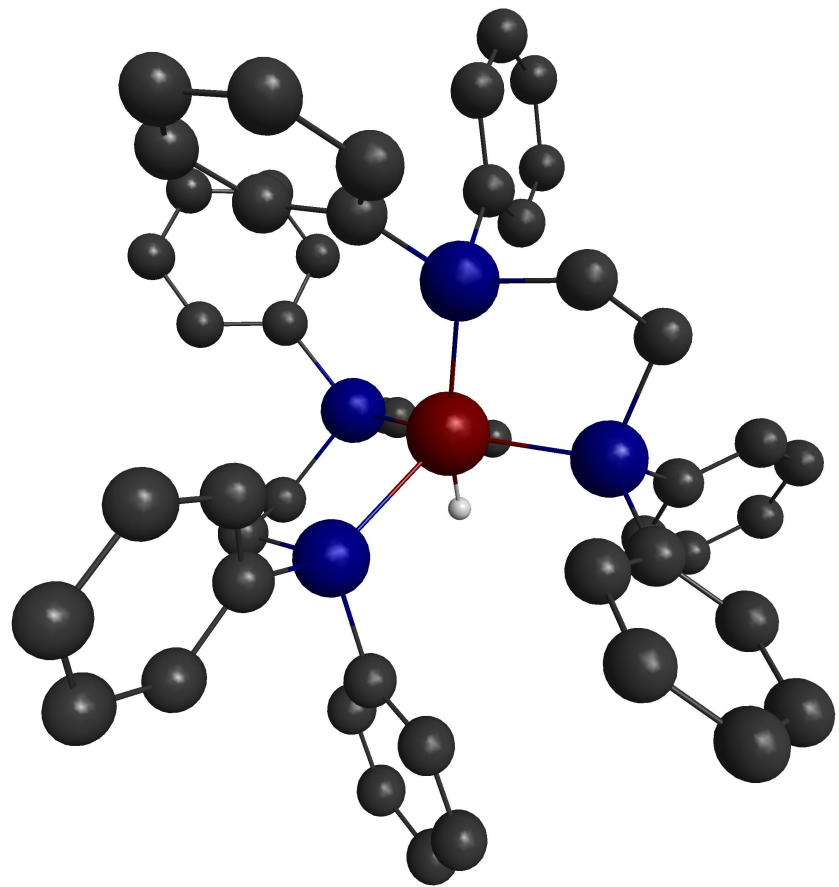


Figure S.4: Optimized structure of the triplet state organometallic $[\text{FeHdppe}_2]^+$ using the UHF approximation and LANL2DZ-ECP basis sets. Structure shows the quasi-square pyramidal structure observed by Franke,¹ et al. Alkyl and aryl hydrogens have been omitted for clarity.

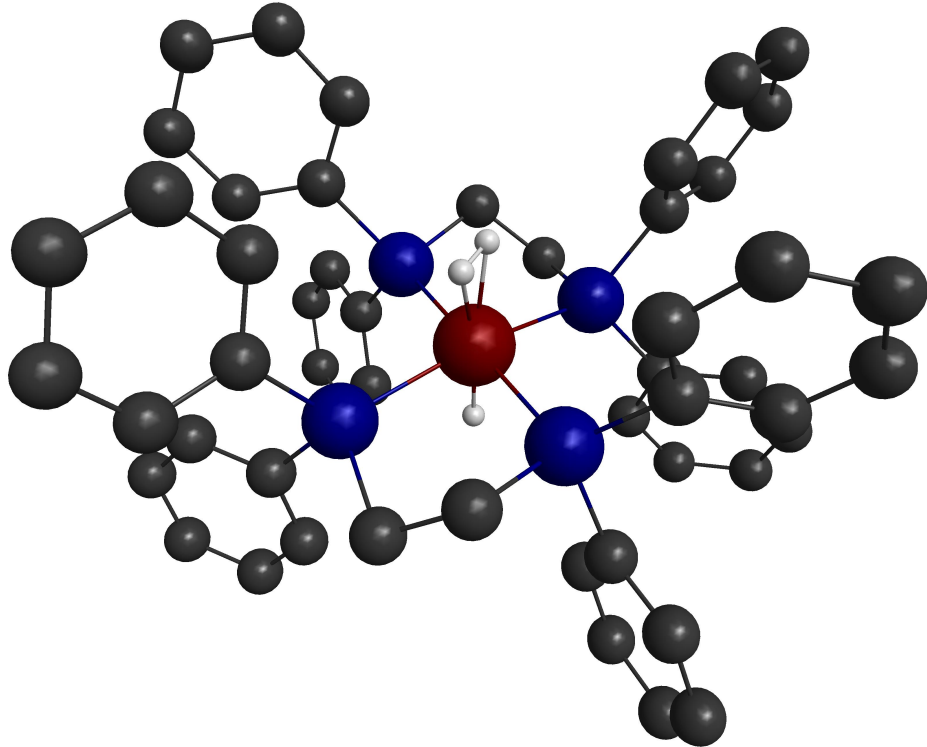


Figure S.5: Optimized structure of $[\text{FeH}(\eta^2\text{-H}_2)\text{dppe}_2]^+$ using the UHF approximation and LANL2DZ-ECP basis sets, showing the octahedral geometry observed from x-ray diffraction measurements.² Alkyl and aryl hydrogens have been omitted for clarity.

Table 1: Calculated values of ground state and vibration energies for molecular fragments as used to calculate the binding energy ΔE . Ground state energies are given using the MP2 level of calculation. Values given are in Hartrees/fragment.

	RHF	ROHF	UHF
<i>H</i> ₂			
ε_0	-1.143887	-1.143887	-1.143887
$\varepsilon_{\text{corr}}$ (295K)	0.012077	0.012077	0.012077
$\varepsilon_{\text{corr}}$ (298K)	0.012101	0.012101	0.012101
$\varepsilon_{\text{corr}}$ (300K)	0.012117	0.012117	0.012117
$\varepsilon_{\text{corr}}$ (313K)	0.012220	0.012220	0.012220
$\varepsilon_{\text{corr}}$ (333K)	0.012378	0.012378	0.012378
$\varepsilon_{\text{corr}}$ (343K)	0.012457	0.012457	0.012457
$\varepsilon_{\text{corr}}$ (353K)	0.012536	0.012536	0.012536
$\varepsilon_{\text{corr}}$ (363K)	0.012615	0.012615	0.012615
$\varepsilon_{\text{corr}}$ (373K)	0.012695	0.012695	0.012695
<i>[FeHdpp<i>e</i>₂]⁺, singlet</i>			
ε_0	-2149.499647	-2149.478130	-2149.499593
$\varepsilon_{\text{corr}}$ (295K)	0.884147	0.884136	0.884016
$\varepsilon_{\text{corr}}$ (298K)	0.885167	0.885157	0.885036
$\varepsilon_{\text{corr}}$ (300K)	0.885853	0.885842	0.885722
$\varepsilon_{\text{corr}}$ (313K)	0.890418	0.890408	0.890288
$\varepsilon_{\text{corr}}$ (333K)	0.897804	0.897795	0.898047
$\varepsilon_{\text{corr}}$ (343K)	0.901659	0.901650	0.901530
$\varepsilon_{\text{corr}}$ (353K)	0.905621	0.905611	0.905491
$\varepsilon_{\text{corr}}$ (363K)	0.909687	0.909677	0.909557
$\varepsilon_{\text{corr}}$ (373K)	0.913855	0.913846	0.913726
<i>[FeHdpp<i>e</i>₂]⁺, triplet</i>			
ε_0	—	-2149.507960	-2149.211701
$\varepsilon_{\text{corr}}$ (295K)	—	0.884384	0.884327
$\varepsilon_{\text{corr}}$ (298K)	—	0.885405	0.884280
$\varepsilon_{\text{corr}}$ (300K)	—	0.886091	0.884960
$\varepsilon_{\text{corr}}$ (313K)	—	0.890659	0.889489
$\varepsilon_{\text{corr}}$ (333K)	—	0.898047	0.896815
$\varepsilon_{\text{corr}}$ (343K)	—	0.901902	0.900639
$\varepsilon_{\text{corr}}$ (353K)	—	0.905863	0.904569
$\varepsilon_{\text{corr}}$ (363K)	—	0.909928	0.908604
$\varepsilon_{\text{corr}}$ (373K)	—	0.914095	0.912741

Table 1 continued

	RHF	ROHF	UHF
<i>[FeH(η^2-H₂)dppe₂]⁺</i>			
ϵ_0	-2150.671333	-2150.671330	-2150.671332
ϵ_{corr} (295K)	0.901449	0.901436	0.901443
ϵ_{corr} (298K)	0.902489	0.902475	0.902482
ϵ_{corr} (300K)	0.903187	0.903174	0.903181
ϵ_{corr} (313K)	0.907839	0.907826	0.907833
ϵ_{corr} (333K)	0.915366	0.915354	0.915360
ϵ_{corr} (343K)	0.919296	0.919283	0.919290
ϵ_{corr} (353K)	0.923333	0.923321	0.923328
ϵ_{corr} (363K)	0.927478	0.927466	0.927472
ϵ_{corr} (373K)	0.931728	0.931716	0.931723
<i>[RuHdppe₂]⁺, singlet</i>			
ϵ_0	-2120.162390	—	—
ϵ_{corr} (295K)	0.884338	—	—
ϵ_{corr} (298K)	0.885284	—	—
ϵ_{corr} (300K)	0.886047	—	—
ϵ_{corr} (313K)	0.890622	—	—
ϵ_{corr} (333K)	0.898020	—	—
ϵ_{corr} (343K)	0.901880	—	—
ϵ_{corr} (353K)	0.905847	—	—
ϵ_{corr} (363K)	0.909918	—	—
ϵ_{corr} (373K)	0.914092	—	—
<i>[RuH(η^2-H₂)dppe₂]⁺</i>			
ϵ_0	-2121.328628	—	—
ϵ_{corr} (295K)	0.900999	—	—
ϵ_{corr} (298K)	0.902042	—	—
ϵ_{corr} (300K)	0.902743	—	—
ϵ_{corr} (313K)	0.907410	—	—
ϵ_{corr} (333K)	0.914960	—	—
ϵ_{corr} (343K)	0.918901	—	—
ϵ_{corr} (353K)	0.922949	—	—
ϵ_{corr} (363K)	0.927105	—	—
ϵ_{corr} (373K)	0.931365	—	—

Table 1 continued

	RHF	ROHF	UHF
<i>[OsHdppe₂]⁺, singlet</i>			
ϵ_0	-2117.324594	—	—
ϵ_{corr} (295K)	0.884733	—	—
ϵ_{corr} (298K)	0.885755	—	—
ϵ_{corr} (300K)	0.886442	—	—
ϵ_{corr} (313K)	0.891014	—	—
ϵ_{corr} (333K)	0.898409	—	—
ϵ_{corr} (343K)	0.902268	—	—
ϵ_{corr} (353K)	0.906233	—	—
ϵ_{corr} (363K)	0.910302	—	—
ϵ_{corr} (373K)	0.914474	—	—
<i>[OsH(η^2-H₂)dppe₂]⁺</i>			
ϵ_0	-2118.506051	—	—
ϵ_{corr} (295K)	0.899768	—	—
ϵ_{corr} (298K)	0.900799	—	—
ϵ_{corr} (300K)	0.901493	—	—
ϵ_{corr} (313K)	0.906110	—	—
ϵ_{corr} (333K)	0.913583	—	—
ϵ_{corr} (343K)	0.917484	—	—
ϵ_{corr} (353K)	0.921493	—	—
ϵ_{corr} (363K)	0.925609	—	—
ϵ_{corr} (373K)	0.929830	—	—

Table 2: SCS-MP2 calculated values of ground state energies for molecular fragments as used to calculate the binding energy ΔE . Calculations were available for the RHF approximation only. Values given are in Hartrees/fragment.

<i>H₂</i>	-1.147356
<i>[FeHdppe₂]⁺, singlet</i>	-2149.376507
<i>[FeH(η^2-H₂)dppe₂]⁺</i>	-2150.544791
<i>[RuHdppe₂]⁺, singlet</i>	-2120.037432
<i>[RuH(η^2-H₂)dppe₂]⁺</i>	-2121.202370
<i>[OsHdppe₂]⁺, singlet</i>	-2117.197672
<i>[OsH(η^2-H₂)dppe₂]⁺</i>	-2118.377019

References

- (1) Franke, O.; Wiesler, B.E.; Lehnert, N.; Peters, G.; Burger, P.; Tuczek, F. *Z. Anorg. Allg. Chem.* **2006**, 632, 1247.
- (2) Morris, R. H.; Sawyer, J. F.; Shiralian, M.; Zubkowski, J. D. *J. Am. Chem. Soc.* **1985**, 107, 5581.